European Journal of Medicinal Chemistry 82 (2014) 204–213

Contents lists available at ScienceDirect

European Journal of Medicinal Chemistry

journal homepage: http://www.elsevier.com/locate/ejmech

Original article

Discovery of HDAC inhibitors with potent activity against multiple malaria parasite life cycle stages

Finn K. Hansen [a], Subathdrage D.M. Sumanadasa [b], Katharina Stenzel [a], Sandra Duffy [b], Stephan Meister [c], Linda Marek [a], Rebekka Schmetter [a], Krystina Kuna [a], Alexandra Hamacher [a], Benjamin Mordmüller [d, e], Matthias U. Kassack [a], Elizabeth A. Winzeler [c], Vicky M. Avery [b], Katherine T. Andrews [b, *, 1], Thomas Kurz [a, *, 1]

[a] Institut für Pharmazeutische und Medizinische Chemie, Heinrich Heine Universität Düsseldorf, Universitätsstr. 1, 40225 Düsseldorf, Germany
[b] Eskitis Institute for Drug Discovery, Don Young Road, Nathan Campus, Griffith University, QLD 4111, Australia
[c] Department of Pediatrics, University of California, San Diego, School of Medicine, 9500 Gilman Drive 0741, La Jolla, CA 92093, USA
[d] Institut für Tropenmedizin, Eberhard Karls Universität Tübingen, Wilhelmstr. 27, 72074 Tübingen, Germany
[e] Medical Research Laboratory, Albert Schweitzer Hospital, Lambaréné, Gabon

ARTICLE INFO

Article history:
Received 30 January 2014
Received in revised form
12 May 2014
Accepted 21 May 2014
Available online 22 May 2014

Dedicated to Prof. Dr. Alan R. Katritzky, in memoriam.

Keywords:
Histone deacetylase inhibitor
Malaria
Liver stages
Asexual blood stages
Gametocyte stages

ABSTRACT

In this work we investigated the antiplasmodial activity of a series of HDAC inhibitors containing an alkoxyamide connecting-unit linker region. HDAC inhibitor **1a** (LMK235), previously shown to be a novel and specific inhibitor of human HDAC4 and 5, was used as a starting point to rapidly construct a mini-library of HDAC inhibitors using a straightforward solid-phase supported synthesis. Several of these novel HDAC inhibitors were found to have potent *in vitro* activity against asexual stage *Plasmodium falciparum* malaria parasites. Representative compounds were shown to hyperacetylate *P. falciparum* histones and to inhibit deacetylase activity of recombinant *Pf*HDAC1 and *P. falciparum* nuclear extracts. All compounds were also screened *in vitro* for activity against *Plasmodium berghei* exo-erythrocytic stages and selected compounds were further tested against late stage (IV and V) *P. falciparum* gametocytes. Of note, some compounds showed nanomolar activity against all three life cycle stages tested (asexual, exo-erythrocytic and gametocyte stages) and several compounds displayed significantly increased parasite selectivity compared to the reference HDAC inhibitor suberoylanilide hydroxamic acid (SAHA). These data suggest that it may be possible to develop HDAC inhibitors that target multiple malaria parasite life cycle stages.

1. Introduction

Despite decades of research on its prevention and treatment, malaria remains a significant disease in tropical and subtropical regions of the world. As reported by the World Health Organization (WHO), 3.3 billion people were at risk of malaria in 2011, which is approximately half of the world's population [1]. In 2010 alone it is estimated that there were ~1.2 million malaria related deaths [2], the vast majority of which were due to infection with *Plasmodium falciparum* parasites. There is currently no licensed malaria vaccine and recent clinical trials in African children with the most advanced candidate, RTS,S/AS02D, were disappointing, with only ~30% protection being achieved over 18 months follow-up [3,4]. Hence, antimalarial drugs currently remain the most effective tool for malaria treatment and, together with vector control strategies, for malaria prophylaxis. Unfortunately, the rapid spread of drug-resistant *P. falciparum* parasites is compromising antimalarial drug efficacy in a clinical setting [5]. Alarming signs of emerging resistance to artemisinin derivatives [6,7] could threaten the now widely-used artemisinin combination therapies (ACTs) and highlight the urgent need to discover and develop new antimalarials with novel modes of action. Drugs that target different, or

Abbreviations: DIC, *N,N′*-diisopropylcarbodiimide; DMF, *N,N*-dimethylformamide; EEF, exo-erythrocytic form; HDAC, histone deacetylase; *Pf*, *Plasmodium falciparum*; *Pf* LSG, *P. falciparum* NF54 late stage gametocytes (IV–V); *Pb*, *Plasmodium berghei*; RT, room temperature; SAHA, suberoylanilide hydroxamic acid; TFA, trifluoroacetic acid; THF, tetrahydrofuran; TSA, trichostatin A.

* Corresponding authors.
E-mail addresses: k.andrews@griffith.edu.au (K.T. Andrews), Thomas.kurz@uni-duesseldorf.de (T. Kurz).

[1] TK and KTA contributed equally to this work as senior authors.

http://dx.doi.org/10.1016/j.ejmech.2014.05.050
0223-5234/

Table 1
Structures and properties of selected hydroxamate-based HDAC inhibitors.

Name	Structure	MW	*P. falciparum* IC_{50} [μM]	Mammalian cell cytotoxicity IC_{50} [μM]	SI[a]
Vorinostat (SAHA)[b]	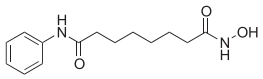	264	0.109–0.309	2.200–>20	7–>183
Trichostatin A (TSA)[b]	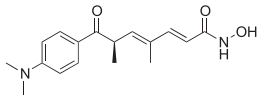	302	0.008–0.011	0.200	18–25
2-ASA-9[b]	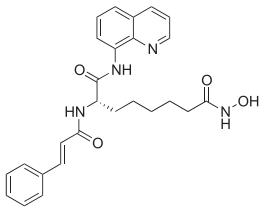	461	0.015–0.039	1.240	32–82
WR301801 (YC-II-88)[c]	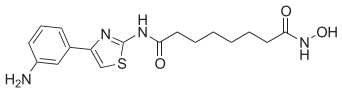	362	0.0006–0.0018	0.600	333–1000
SB939[d]	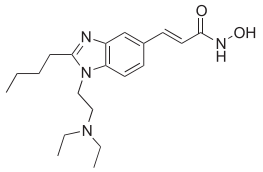	358	0.080–0.150	0.800–>100	4–>1250

[a] SI = (mammalian cell IC_{50})/(*P. falciparum* IC_{50}) – larger values indicate greater malaria parasite selectivity.
[b] Data from Ref. [25].
[c] Data from Ref. [28].
[d] Data from Ref. [29].

preferably multiple, parasite life cycle stages are also a high priority. Most current antimalarials are active against the asexual blood stages of the parasite, which are responsible for the clinical symptoms of malaria [1]. However, recent drug discovery efforts have moved towards eradication of malaria [8], and seek to additionally target exo-eryothrocytic liver stages and gametocyte (transmission) stage parasites [9]. *Plasmodium* liver stages are clinically silent pre-erythrocytic life cycle stages that are promising targets for new drugs as inhibition of this stage leads to a true causal prophylaxis [10]. The transmission of malaria parasites to the female *Anopheles* mosquito vector occurs when sexual stage gametocytes are taken up in the blood of an infected individual during a blood meal. Following fertilization, meiosis and sporogony in the mosquito, progeny parasites can then be transmitted to another host when the female mosquito feeds again. A considerable number of drugs, which kill asexual parasites and alleviate symptoms, do not kill late stage gametocytes, allowing the infected individual to continue to spread the disease even after symptoms have disappeared [11]. Therefore, therapeutically blocking transmission is also a high priority for the malaria elimination agenda [11,12].

One promising strategy to identify new antimalarial agents is the "piggyback" approach, which focuses on drug targets that have been validated for other diseases. Using this approach, we, and others, have previously investigated the antimalarial potential of compounds that target histone deacetylase (HDAC) enzymes [13,14]. While no HDAC inhibitor has yet been used clinically for malaria, this class of compound has been progressed to clinical use for cancer. Both the hydroxamate-based pan-HDAC inhibitor, vorinostat (suberoylanilide hydroxamic acid (SAHA)), and the class I selective prodrug, romidepsin (FK228), have been approved for treatment of cutaneous T-cell lymphoma (CTCL) [15–21]. The *P. falciparum* genome contains at least five putative HDACs [22] and the enzyme *P. falciparum* histone deacetylase 1 (*Pf*HDAC1) has been identified as a target of antimalarial HDAC inhibitors [23]. Treatment of *P. falciparum* parasites with HDAC inhibitors results in genome wide transcriptional alterations [24–26] and altered *Pf*HDAC1 expression has been found in *P. falciparum* parasite lines with reduced clinical susceptibility to artemisinin [27]. Together these findings underscore *Pf*HDACs' potential as novel parasite drug targets. The structures and properties of selected hydroxamate-based HDAC inhibitors with antimalarial activity are summarized in Table 1.

Despite some progress in recent years, there are still a number of challenges in the rational development of HDAC inhibitors as antimalarial drug leads. Next generation compounds should retain potent antiplasmodial activity and low host cell toxicity, but they also require improved pharmacokinetic properties relative to current generation compounds. In addition, while most work to date has focused on asexual stage parasites [13], we recently showed that two HDAC inhibitors (SAHA and SB939; see Table 1 for structures) have potent activity (IC_{50} ~150 nM) against exo-erythrocytic stage *Plasmodium* parasites [29]. This raises the possibility that HDAC inhibitors could be developed as causal prophylactic and/or transmission blocking agents.

In this work we investigated the antimalarial activity of a new type of HDAC inhibitor, containing an alkoxyamide connecting-unit linker region [30], against different parasite life cycle stages. Previous work on the cytotoxicity and HDAC inhibitory activity of these alkoxyamide-based HDAC inhibitors against different human cisplatin sensitive and

resistant cancer cell lines revealed potent cytotoxic properties and led to the discovery of **1a** (LMK235). Compound **1a** (LMK235) has a unique selectivity toward human HDAC4 and 5, which are inhibited with low nanomolar IC_{50} values [30]. To determine if this new type of HDAC inhibitor has antimalarial potential, we investigated the antimalarial activity of **1a** (LMK235) and a panel of analogues generated via solid-phase supported synthesis. All compounds were tested for *in vitro* activity against asexual stage *P. falciparum* parasites, exo-erythrocytic *Plasmodium* parasites cultured in HepG2 liver cells and for cytotoxicity against HepG2 liver cells. Selected compounds were then examined for gametocytocidal properties as well as inhibition of *Pf*HDAC1 enzyme activity and the ability to hyperacetylate histones in asexual stage *P. falciparum* parasites.

2. Results and discussion

2.1. Synthesis

The conventional synthesis of compounds **1a**–**h** was published previously [30]. In order to obtain a more rapid and convenient access to alkoxyamide-based HDAC inhibitors of type **1**, we developed the 5-step solid-phase synthesis illustrated in Scheme 1. The commercially available Fmoc-hydroxylamine-2-chlorotrityl resin **2** was chosen as suitable solid support. First, the polymer-bound phthaloyl-protected linker **3** was prepared in two steps by deprotection of the Fmoc group and subsequent acylation of the free hydroxylamine moiety with 6-((1,3-dioxoisoindolin-2-yl)oxy)hexanoic acid (4 equiv.) using DIC/Oxyma (4 equiv.) as coupling agents. Subsequently, the phthaloyl protection was cleaved with methylhydrazine to provide the resin-bound key intermediate **4**, which allowed the solid-phase synthesis of the alkoxyamide-based HDAC inhibitors **1i**–**u**. Our mini library of HDAC inhibitors was prepared using resin **4** and 13 different benzoic acid derivatives. First, the desired cap group (3 equiv.) was introduced by DIC/Oxyma-mediated (3 equiv.) amide coupling reaction to give the resin-bound HDAC inhibitors **5i**–**u**. The DIC/Oxyma system in the absence of a base was chosen to prevent any possible *N*-overacylation of the NH–O function, which is a well-known side reaction in the synthesis of aminoxy-based compounds particularly observed under solid-phase reaction conditions [31–34]. Finally, HDAC inhibitors **1i**–**u** were conveniently released from the resin by treatment of **5i**–**u** with 5% trifluoroacetic acid (TFA) in dichloromethane. Purification by flash column chromatography provided the target compounds **1i**–**u** in 14–36% overall yields (over five steps).

2.2. In vitro activity against P. falciparum asexual blood stages

The antimalarial activity of alkoxyamide-based HDAC inhibitors **1a**–**u** was first tested against asexual-stage *P. falciparum* parasites using a tritiated hypoxanthine incorporation assay. Based on calculated physicochemical properties, all compounds were within the limits of Lipinski's rule of five [35] and were thus expected to be cell permeable (see Table 2 for calculated log *P* values). When tested for *in vitro* activity against the chloroquine-sensitive *P. falciparum* 3D7 line, 50% inhibitory concentration values (IC_{50}s) were in the range of 0.09–1.12 μM (Table 2). Compound **1i** was the most active compound in this series (*R* = 4-*t*-Bu-Ph, *Pf* 3D7 IC_{50}: 0.09 μM). Apparently, derivatives bearing alkyl groups in *m*- or *p*-position of the phenyl core exhibited more potent activity compared to the *o*-methyl derivative **1h** (IC_{50}: 1.12 μM). Interestingly, the dimethylphenyl-substituted compounds were more active than their respective mono-methyl counterparts. The potency increases with the bulkiness of the alkyl group in *p*-position (4-*t*-Bu-Ph (**1i**) > 4-*i*-Pr-Ph (**1c**) > 4-CH_3-Ph (**1e**); Table 2). A similar pattern is observed for the alkoxy-substituted compounds, where the 4-isopropoxyphenyl derivative **1j** (IC_{50}: 0.15 μM) showed the highest activity against *P. falciparum*. It is worth noting that introducing a (1,1′-biphenyl)-4-yl cap group, as in **1k**, does not significantly alter the activity (IC_{50}: 0.16 μM), which indicates that bulky substituents are well tolerated.

2.3. Cytotoxicity and selectivity indices

To assess the selectivity of alkoxyamide-based HDAC inhibitors for the parasite versus mammalian cells, cytotoxicity was evaluated against HepG2 liver cells. The results and selectivity indices (SIs) are outlined in Table 2. All compounds with a methyl group in *m*-position of the phenyl ring showed only moderate parasite selectivity (SI: 13–27). However, several other compounds revealed significantly increased selectivity for the parasite compared to the reference HDAC inhibitor SAHA (SI: 11, Table 2). As already observed for the activity against asexual blood stages, the parasite selectivity increases with the bulkiness of the alkyl group in *p*-position (4-*t*-Bu-Ph (**1i**, SI: 139) > 4-*i*-Pr-Ph (**1c**, SI: 73) > 4-CH_3-Ph (**1e**, SI: 55); Table 2). In addition, the bulky biphenyl-based compound **1k** (SI: 64) showed increased selectivity for the parasite compared to SAHA (SI: 11). The selectivity indices of the alkoxy-substituted compounds are particularly interesting. The 2- and 3-propoxy-substituted compounds (**1p** and **1q**, SI: 34 and 29, respectively) are significantly less parasite selective than the 4-propoxy analogue **1m** (SI: 80). The truncated 4-ethoxy derivative **1o** (SI: 33) displayed a decreased selectivity index compared to **1m**. Remarkably, all elongated alkoxy compounds showed no cytotoxicity at the highest concentration tested (50 μM) and the butoxy- (**1l**), pentoxy- (**1n**) and hexoxy-substituted (**1s**) HDAC inhibitors revealed promising selectivity indices with >294, >238 and >143, respectively. These data indicate that the introduction of bulky- and alkoxy-substituted cap groups on HDAC inhibitors of type **1** might

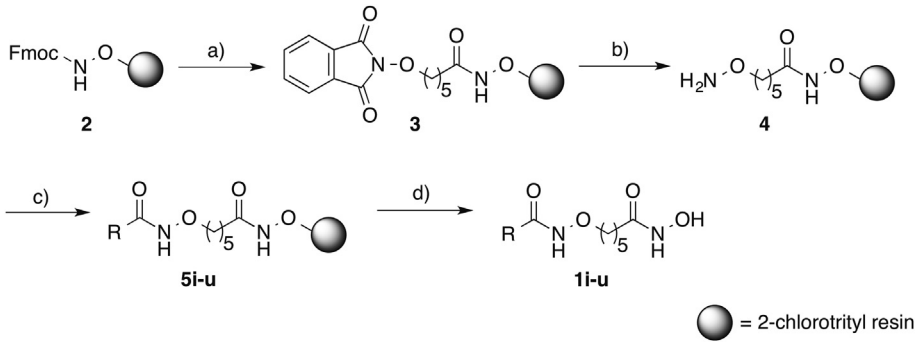

Scheme 1. Solid-phase synthesis of alkoxyamide-based HDAC inhibitors **1i**–**u**. Reagents and conditions: a) (i) piperidine, DMF, RT, 1 h; (ii) 6-((1,3-dioxoisoindolin-2-yl)oxy)hexanoic acid, DIC, Oxyma, CH_2Cl_2, RT, 24 h; b) methylhydrazine, ethanol, THF, RT, 3 h; c) RCOOH, DIC, Oxyma, CH_2Cl_2, RT, 24 h; d) TFA, CH_2Cl_2, RT, 1 h.

Table 2
Calculated log *P* values, *in vitro* activity against asexual blood stages of *P. falciparum* 3D7 parasites, cytotoxicity and selectivity indices of **1a**–**1u**.

Compound	R	Log *P*[a]	*Pf* 3D7[b] IC_{50} [μM]	HepG2 IC_{50} [μM]	95% CI for HepG2 IC_{50}	SI[c]
1a	3,5-CH_3-Ph	2.05 (±0.57)	0.10 (±0.02)	1.26	1.06–1.51	13
1b	3,4-CH_3-Ph	2.05 (±0.57)	0.12 (±0.03)	3.24	2.50–4.19	27
1c	4-*i*-Pr-Ph	2.47 (±0.57)	0.12 (±0.02)	8.76	5.68–13.51	73
1d	3-CH_3-Ph	1.59 (±0.56)	0.19 (±0.06)	4.69	3.83–5.73	25
1e	4-CH_3-Ph	1.59 (±0.56)	0.22 (±0.02)	12.11	8.49–17.28	55
1f	4-CF_3-Ph	2.10 (±0.58)	0.26 (±0.03)	12.96	10.33–16.27	50
1g	4-F-Ph	1.35 (±0.59)	0.58 (±0.14)	10.33	8.33–12.81	18
1h	2-CH_3-Ph	1.59 (±0.56)	1.12 (±0.19)	12.74	10.19–15.94	11
1i	4-*t*-Bu-Ph	2.82 (±0.57)	0.09 (±0.03)	12.47	7.24–21.47	139
1j	4-*i*-PrO-Ph	2.17 (±0.57)	0.15 (±0.03)	9.76	7.00–13.61	65
1k	4-Ph′-Ph	2.77 (±0.58)	0.16 (±0.03)	10.24	8.66–12.10	64
1l	4-BuO-Ph	2.89 (±0.57)	0.17 (±0.03)	>50		>294
1m	4-PrO-Ph	2.36 (±0.57)	0.21 (±0.02)	16.86	10.92–26.06	80
1n	4-$C_5H_{11}O$-Ph	3.42 (±0.57)	0.21 (±0.04)	>50		>238
1o	4-C_2H_5O-Ph	1.82 (±0.57)	0.23 (±0.05)	7.68	4.68–12.61	33
1p	2-PrO-Ph	1.92 (±0.57)	0.24 (±0.02)	8.12	4.64–14.23	34
1q	3-PrO-Ph	2.36 (±0.57)	0.24 (±0.04)	7.04	4.27–11.59	29
1r	4-Bu-Ph	3.18 (±0.56)	0.26 (±0.08)	10.77	7.71–15.03	41
1s	4-$C_6H_{13}O$-Ph	3.95 (±0.57)	0.35 (±0.05)	>50		>143
1t	furan-2-yl	−0.08 (±0.58)	0.62 (±0.16)	8.03	6.04–10.69	13
1u	2-F-Ph	0.76 (±0.59)	0.73 (±0.05)	9.10	6.96–11.89	12
SAHA		0.86 (±0.21)	0.13 (±0.02)[d]	1.49	0.97–2.29	11
Chloroquine		4.69 (±0.32)	0.01 (±0.006)	>10		>1000

[a] LogP values were calculated using ACD/ChemSketch freeware version 12.01.
[b] Three independent assays, each carried out in triplicate wells.
[c] SI = (mammalian cell IC_{50})/(*P. falciparum* IC_{50}) – larger values indicate greater malaria parasite selectivity.
[d] Data from Ref. [36]. CI, confidence interval.

be a useful tool for the development of antimalarial lead compounds with potent and selective action against *P. falciparum*.

2.4. Mode of action of alkoxyamide-based HDAC inhibitors in asexual-stage P. falciparum parasites

The mode of action of eight representative alkoxyamide-based HDAC inhibitors in asexual-stage parasites was assessed by examining *in situ* hyperacetylation of *P. falciparum* histones and *in vitro* activity against *P. falciparum* nuclear lysates and recombinant *Pf*HDAC1. Like the control compound TSA, **1a**–**1d** and **1i**–**1l** caused hyperacetylation of *P. falciparum* histone H4 (Fig. 1). Histone H3 was also hyperacetylated by all eight compounds, although apparently to a lesser extent by **1b** (Fig. 1). The reason for this is not yet know, however the effect was not due to unequal loading, as the same membrane was also probed with control antisera (anti-IC3/94) to confirm equivalent protein levels were present.

Compounds **1a**–**d** and **1i**–**1l** were also tested for their ability to inhibit deacetylase activity in *P. falciparum* nuclear lysates and the activity of recombinant *Pf*HDAC1. All compounds displayed >50% inhibition of *Pf*HDAC1 activity at 1 μM and all but **1j** > ~50% inhibition of *P. falciparum* nuclear extract at 1 μM (Table 3). The reason for a lack of deacetylase inhibition by **1j** is not yet known, however compound stability can be ruled out, as this compound was still active in the other mode of action assays (Fig. 1; Table 3). Once additional recombinant *Pf*HDAC proteins become available it will be important to profile this compound and other HDAC inhibitors against different malaria HDAC enzymes.

2.5. In vitro activity against tissue schizontocidal stages of P. berghei

We showed previously that two commercially available HDAC inhibitors, SAHA and SB939, can potently inhibit exo-erythrocytic stage *Plasmodium berghei* parasite development *ex vivo* in HepG2 liver cells (IC_{50} ~ 0.15 μM) [29]. This prompted us to assess the activity of our novel HDAC inhibitors against this life cycle stage. Five of 21 compounds tested (**1a**, **1b**, **1d**, **1p** and **1q**) displayed potent activity against *P. berghei* exo-erythrocytic stages with IC_{50} values ranging from 0.16 to 0.66 μM, 13 had moderate activity with

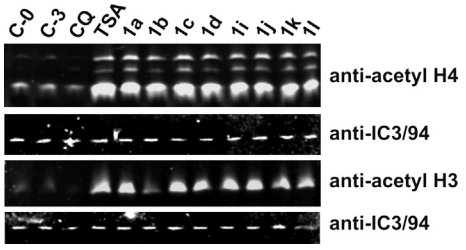

Fig. 1. Hyperacetylation of *P. falciparum* histones. Trophozoite-stage *P. falciparum* 3D7 parasites were treated for 3 h with 500 nM chloroquine (**CQ**), **TSA**, or compounds **1a**–**1d** or **1i**–**1l**. Parasites treated with vehicle only (0.05% DMSO) served as negative controls and were taken at the start of the treatment (**C-0**) and after 3 h (**C-3**). Protein lysates were analysed by Western blot with antisera that recognize tetra-acetylated histone H4 (**anti-acetyl H4**) or N-terminally acetylated histone H3 (**anti-acetyl H3**). In each case the same membranes were also probed with antisera that recognizes *P. falciparum* RAP2 (anti-IC3/94) to show equivalent loading between lanes.

Table 3
Inhibition of *P. falciparum* nuclear lysates and recombinant *Pf*HDAC1.

Compound	R	*Pf* nuclear lysate % inhibition at 1 μM[a]	*Pf* HDAC1% inhibition at 1 μM[a]
1a	3,5-CH_3-Ph	58.6 (±12.5)	73.8 (±7.5)
1b	3,4-CH_3-Ph	93.3 (±2.4)	82.6 (±4.2)
1c	4-*i*-Pr-Ph	72.9 (±10.4)	67.2 (±0.5)
1d	3-CH_3-Ph	73.9 (±16.3)	75.5 (17.8)
1i	4-*t*-Bu-Ph	48.3 (±7.3)	68.6 (±1.2)
1j	4-*i*-PrO-Ph	9.3 (±4.6)	62.4 (±10.1)
1k	4-Ph′-Ph	89.3 (±0.2)	64.2 (±19.4)
1l	4-BuO-Ph	50.3 (±11.5)	72.1 (±5.0)
TSA		78.1 (±12.6)	93.3 (±10.9)

[a] Average (±SD) of two independent assays, each carried out in duplicate wells.

Table 4
Activity of alkoxyamide-based HDAC inhibitors against *P. berghei* exo-erythrocytic stages.

Compound	R	*Pb* EEF[a] IC_{50} [μM]	95% CI for *Pb* EEF IC_{50}	HepG2 IC_{50} [μM]	95% CI for HepG2 IC_{50}	EEF SI[b]
1a	3,5-CH_3-Ph	0.16	0.12–0.21	1.26	1.06–1.51	8
1b	3,4-CH_3-Ph	0.31	0.23–0.42	3.24	2.50–4.19	10
1c	4-*i*-Pr-Ph	1.34	0.68–2.62	8.76	5.68–13.51	7
1d	3-CH_3-Ph	0.66	0.50–0.87	4.69	3.83–5.73	7
1e	4-CH_3-Ph	1.14	0.78–1.69	12.11	8.49–17.28	11
1f	4-CF_3-Ph	1.90	1.22–2.96	12.96	10.33–16.27	7
1g	4-F-Ph	2.31	1.46–3.64	10.33	8.33–12.81	4
1h	2-CH_3-Ph	2.54	1.68–3.86	12.74	10.19–15.94	5
1i	4-*t*-Bu-Ph	1.87	1.65–2.12	12.47	7.24–21.47	7
1j	4-*i*-PrO-Ph	1.36	0.86–2.13	9.76	7.00–13.61	7
1k	4-Ph′-Ph	1.83	1.51–2.22	10.24	8.66–12.10	6
1l	4-BuO-Ph	2.14	1.14–4.01	>50		>23
1m	4-PrO-Ph	~5.29	(Very wide)	16.86	10.92–26.06	~3
1n	4-$C_5H_{11}O$-Ph	~5.14	(Very wide)	>50		>10
1o	4-C_2H_5O-Ph	1.37	0.86–2.18	7.68	4.68–12.61	6
1p	2-PrO-Ph	0.48	0.32–0.72	8.12	4.64–14.23	17
1q	3-PrO-Ph	0.45	0.30–0.68	7.04	4.27–11.59	16
1r	4-Bu-Ph	~1.79	(Very wide)	10.77	7.71–15.03	~6
1s	4-$C_6H_{13}O$-Ph	7.91	4.60–13.62	>50		>6
1t	furan-2-yl	1.13	0.72–1.78	8.03	6.04–10.69	7
1u	2-F-Ph	1.25	0.68–2.28	9.10	6.96–11.89	7
SAHA		0.14	0.11–0.20	1.49	0.97–2.29	11
Chloroquine		>10		>10		–
Atovaquone		0.00016	0.000085–0.00028	>10		>64,102

[a] *P. berghei* exo-erythrocytic forms (EEF).
[b] SI = (mammalian cell IC_{50})/(*Pb* EEF IC_{50}) – larger values indicate greater malaria parasite selectivity. CI, confidence interval.

IC_{50}s between 1.13 and 2.54 μM, while three (**1m**, **1n** and **1s**) showed no activity with IC_{50} values > 5 μM (Table 4). Remarkably, the most active compounds all bear a methyl group in the 3-position of the phenyl ring (**1a**, **1b**, and **1d**) or a propoxy group in 2- or 3-position (**1p** and **1q**).

A comparison of the IC_{50} values for *P. berghei* exo-erythrocytic stages with those obtained for HepG2 liver cells indicate a moderate parasite-specific selectivity for compounds with sub-μM IC_{50}s (SI: ~7 –17; Table 4). These selectivity indices are comparable with the selectivity of the reference compound SAHA (SI: 11, Table 4). Some of the alkoxysubstituted derivatives in this study were not cytotoxic at the highest concentration tested (50 μM) indicating that it should be possible to develop parasite-specific HDAC inhibitors that selectively target exo-erythrocytic stage parasites. In particular compound **1l** (SI: > 23) will be the subject of future work to determine if this compound has potential as chemical starting point for exo-erythrocytic stage drug development.

2.6. In vitro activity against late stage gametocytes

There is an increasing focus on the elimination, rather than just prevention and treatment, of malaria and to achieve this it will be important to identify approaches to block the transmission of sexual (gametocyte) stage *Plasmodium* parasites to the mosquito vector. When we examined the activity of a sub-set of our alkoxyamide-based HDAC inhibitors against late-stage gametocytes (see Table 5), we found that five of nine compounds tested (**1a**, **1b**, **1d**, **1k** and **1t**) had IC_{50} values ≤1 μM, two had less potent activity with IC_{50} values between 2.0 and 5.3 μM (**1g** and **1r**) while two (**1i** and **1u**) were not active (IC_{50} > 120 μM). As already observed for *P. berghei* exo-erythrocytic stages, a 3-methylphenyl substitution emerges as beneficial, as indicated by the potent activities of compounds **1a**, **1b**, and **1d** with IC_{50}s between 0.25 and 0.43 μM. Notably, compound **1b**, bearing a methyl group in *m*- and *p*-position, was the most active compound of this series (IC_{50} 0.25 μM). Interestingly, compound **1k** displayed good activity against late-stage gametocytes (IC_{50} 0.50 μM). Hence, biphenyl-based HDAC inhibitors appear to be interesting scaffolds for the development of antimalarials with activity against sexual (gametocyte) stages.

A comparison of the IC_{50} values of the four most potent compounds with those obtained for HepG2 cells (Table 2) indicates that **1a** is cytotoxic (SI: 4), while **1b** has around 13 fold, **1d** 11 fold and **1k** 20 fold more activity against late stage gametocytes versus mammalian cells. It is interesting to note that **1k** showed only moderate activity against exo-erythrocytic stages (*Pb* EEF IC_{50}: 1.83 μM, Table 4). As we do not yet know which *Pf*HDACs are expressed in different life cycle stages, or their relative abundance, such differences in activity could be due to differences in HDAC isoform expression. Alternatively, differences could also be due to the use of different species of parasites in the respective assays (*P. berghei* versus *P. falciparum*). It is also possible that the differences we see are due to interference with the regulation of HDAC-

Table 5
Activity of alkoxyamide-based HDAC inhibitors against stage IV–V *P. falciparum* gametocytes.

Compound	R	*Pf* LSG[a] IC_{50} [μM]
1a	3,5-CH_3-Ph	0.33[b] (±0.01)
1b	3,4-CH_3-Ph	0.25[b] (±0.10)
1d	3-CH_3-Ph	0.43[b] (±0.1)
1g	4-F-Ph	2.0[b] (±0.01)
1i	4-*t*-Bu-Ph	>120[c,d]
1k	4-Ph′-Ph	0.50[b] (±0.14)
1r	4-Bu-Ph	5.3[c]
1t	furan-2-yl	1.0[b] (±0.2)
1u	2-F-Ph	>120[c,d]
Artesunate		0.0038 (±0.0003)[b]
Pyronaridine		2.7 (±0.87)[e]
Chloroquine		>120[b]

[a] *P. falciparum* NF54 late stage gametocytes (IV–V).
[b] *n* = 2, each in duplicate wells.
[c] *n* = 1, each in duplicate wells.
[d] No activity at 120 μM.
[e] *n* = 7, each in duplicate wells. *nd*, not determined.

associated stage-specific proteins or pathways, or even to action against alternative molecular targets.

3. Conclusions

Starting from **1a** (LMK235), a specific inhibitor of human HDAC4 and 5, we have now extended our studies to examine the activity of **1a** and novel structural analogues against malaria parasites. For this purpose, we developed a straightforward solid-phase synthesis allowing the rapid construction of mini libraries of HDAC inhibitors with an alkoxyamide connecting-unit linker region. Biological evaluation of a panel of 21 alkoxyamide-based HDAC inhibitors against the chloroquine-sensitive 3D7 line of *P. falciparum* revealed IC_{50} values in the range of 0.09–1.12 μM. Modification of the cap group showed that the nature of the substitution on the phenyl ring is crucial for the parasite selectivity. All compounds were tested *in vitro* for their activity against tissue schizontocidal stages of *P. berghei* (exo-erythrocytic forms) and selected compounds were further tested against sexual stage *P. falciparum* parasites (stage IV/V gametocytes). Notably, compounds **1a** (LMK235), **1b** and **1d** showed nanomolar activity against all three life cycle stages, while other compounds revealed increased parasite selectivity in combination with at least dual-stage activity. Thus, this series of compounds represents a valuable starting point for the development of novel antimalarial drug leads with potent antiplasmodial activity against multiple malaria parasite life cycle stages, low host cell toxicity, and causal prophylactic and/or transmission blocking properties.

4. Experimental section

4.1. Synthesis

All solvents and chemicals were used as purchased without further purification. Column chromatography was performed with Macherey–Nagel silica gel 60 M (0.04–0.063 mm). TLC analysis was performed on Merck precoated silica gel plates (with fluorescence indicator UV_{254}). Spots were visualized by irradiation with ultraviolet light (254 nm). Melting points (mp) were taken in open capillaries on a Mettler FP 5 melting-point apparatus and are uncorrected. Proton (^1H) and carbon (^{13}C) NMR spectra were recorded on a Bruker Avance 500 (500.13 MHz for ^1H; 125.76 MHz for ^{13}C) using DMSO-d_6 as solvent. Chemical shifts are given in parts per million (ppm), (δ relative to residual solvent peak for ^1H and ^{13}C or to tetramethylsilane). Elemental analysis was performed on a Perkin Elmer PE 2400 CHN elemental analyzer. IR spectra were recorded on a Varian 800 FT-IR Scimitar series. HRMS analysis was performed on a UHR-TOF maXis 4G, Bruker Daltonics, Bremen. HPLC purity determination was carried out using a Phenomenex Luna C-18(2) 1.8 μm particle (250 mm × 4.6 mm) column, supported by Phenomenex Security Guard Cartridge Kit C18 (4.0 mm × 3.0 mm). The purity of all final compounds was 95% or higher. Fmoc-hydroxylamine-2-chlorotrityl resin was purchased from Iris Biotech, Germany. All solid phase reactions were carried out in a Heidolph Synthesis 1 parallel synthesizer. 3-Propoxybenzoic acid [37] and 6-((1,3-dioxoisoindolin-2-yl)oxy) hexanoic acid [30] were prepared according to literature.

4.2. General procedures for solid-phase synthesis

4.2.1. General procedure for the coupling of 6-((1, 3-dioxoisoindolin-2-yl) oxy) hexanoic acid to the resin

Fmoc-hydroxylamine-2-chlorotrityl resin (500 mg, 0.4 mmol, Iris Biotech) was treated with 20% piperidine in DMF (1 × 10 mL, 1 h) and washed with CH_2Cl_2 (3 × 10 mL). A solution of 6-((1, 3-dioxoisoindolin-2-yl) oxy) hexanoic acid (443 mg, 1.6 mmol), Oxyma (227 mg, 1.6 mmol) and DIC (202 mg, 1.6 mmol) in CH_2Cl_2 (10 mL) was added and the resin was shaken for 24 h at room temperature. Afterward, the resin was drained and washed with CH_2Cl_2 (3 × 5 mL), MeOH (3 × 5 mL), CH_2Cl_2 (3 × 5 mL).

4.2.2. General procedure for the removal of the phthaloyl-protection group

The resin was suspended in EtOH:THF (1:1, 10 mL) and methylhydrazine (1.5 mL, 28.7 mmol) was added. Subsequently, the resin was shaken at room temperature (3 h). The resin was drained and washed with MeOH (3 × 5 mL), THF (3 × 5 mL), CH_2Cl_2 (3 × 5 mL).

4.2.3. General procedure for the coupling of benzoic acid derivatives

A solution of the respective carboxylic acid (1.2 mmol), Oxyma (171 mg, 1.2 mmol) and DIC (151 mg, 1.2 mmol) in CH_2Cl_2 (10 mL) was added to the resin and shaken for 24 h. The resin was washed with CH_2Cl_2 (3 × 5 mL), MeOH (3 × 5 mL), CH_2Cl_2 (3 × 5 mL).

4.2.4. General procedure for the cleavage of resin-bound HDAC inhibitors

The resin was treated with 5% TFA in CH_2Cl_2 (1 × 10 mL) at room temperature (1 h). The resin was drained and washed with CH_2Cl_2 (3 × 5 mL). The filtrates were combined and evaporated to dryness under reduced pressure. The crude products were purified by column chromatography using hexane/ethyl acetate (gradient) as eluent to afford the desired HDAC inhibitors.

4.3. Experimental data

4.3.1. 4-(Tert-butyl)-N-((6-(hydroxyamino)-6-oxohexyl)oxy) benzamide (**1i**)

White solid; yield 22%; mp 46 °C. ^1H NMR (500.13 MHz, DMSO-d_6): δ = 11.54 (s, 1H), 10.36 (s, 1H), 8.68 (s, 1H), 7.68 (d, J = 8.4 Hz, 2H), 7.48 (d, J = 8.4 Hz, 2H), 3.85 (t, J = 6.4 Hz, 2H), 1.96 (t, J = 7.3 Hz, 2H), 1.64–1.48 (m, 4H), 1.41–1.22 (m, 11H) ppm. ^{13}C NMR (125.76 MHz, DMSO-d_6): δ = 168.89, 164.01, 154.22, 129.54, 126.78, 125.08, 74.96, 34.52, 32.08, 30.79, 27.34, 24.98, 24.81 ppm. IR (KBr): $\tilde{\nu}$ = 3200 (NH), 2954, 2873 (CH_2), 1642 (C=O) cm^{-1}. HRMS (ESI) $[M + H]^+$: 323.19656, Calcd. for $C_{17}H_{27}N_2O_4$: 323.19653. HPLC analysis: retention time = 14.18 min; peak area: 97.86%. Eluent A: 5 mM NH_4OAc solution; eluent B: CH_3CN, gradient (95:5–> 5:95) over 20 min at a flow rate of 1.0 mL min^{-1}.

4.3.2. N-((6-(Hydroxyamino)-6-oxohexyl)oxy)-4-isopropoxybenzamide (**1j**)

White solid; yield 23%; mp 125 °C. ^1H NMR (500.13 MHz, DMSO-d_6): δ = 11.45 (s, 1H), 10.36 (s, 1H), 8.68 (s, 1H), 7.69 (d, J = 8.7 Hz, 2H), 6.96 (d, J = 8.7 Hz, 2H), 4.76–4.64 (m, 1H), 3.84 (t, J = 6.4 Hz, 2H), 1.96 (t, J = 7.3 Hz, 2H), 1.65–1.48 (m, 4H), 1.44–1.30 (m, 2H), 1.27 (d, J = 6.0 Hz, 6H) ppm. ^{13}C NMR (125.76 MHz, DMSO-d_6): δ = 168.92, 163.81, 159.96, 128.81, 124.00, 114.87, 74.96, 69.25, 32.10, 27.36, 25.00, 24.82, 21.59 ppm. IR (KBr): $\tilde{\nu}$ = 3358, 3181 (NH), 2938, 2868 (CH_2), 1666 (C=O) cm^{-1}. Anal. Calcd. for $C_{16}H_{24}N_2O_5$: C 59.24, H 7.46, N 8.64. Found: C 59.30, H 7.74, N 8.36.

4.3.3. N-((6-(Hydroxyamino)-6-oxohexyl)oxy)-[1,1′-biphenyl]-4-carboxamide (**1k**)

White solid; yield 27%; mp 155 °C. ^1H NMR (500.13 MHz, DMSO-d_6): δ = 11.69 (s, 1H), 10.37 (s, 1H), 8.69 (s, 1H), 7.89–7.82 (m, 2H), 7.80–7.75 (m, 2H), 7.75–7.69 (m, 2H), 7.53–7.47 (m, 2H), 7.44–7.38 (m, 1H), 3.89 (t, J = 6.4 Hz, 2H), 1.98 (t, J = 7.3 Hz, 2H), 1.66–1.50 (m, 4H), 1.43–1.31 (m, 2H) ppm. ^{13}C NMR (125.76 MHz, DMSO-d_6): δ = 168.91, 163.73, 142.95, 138.96, 131.08, 128.93, 128.01, 127.62, 126.75, 126.53, 75.04, 32.10, 27.36, 24.99, 24.82 ppm. IR (KBr):

$\tilde{\nu}$ = 3222 (NH), 2942, 2862 (CH_2), 1648 (C=O) cm^{-1}. Anal. Calcd. for $C_{19}H_{22}N_2O_4$: C 66.65, H 6.48, N 8.18. Found: C 66.50, H 6.33, N 8.09.

4.3.4. 4-Butoxy-N-((6-(hydroxyamino)-6-oxohexyl)oxy)benzamide (**1l**)

White solid; yield 18%; mp 125 °C. ^{1}H NMR (500.13 MHz, DMSO-d_6): δ = 11.46 (s, 1H), 10.36 (s, 1H), 8.67 (s, 1H), 7.70 (d, J = 8.7 Hz, 2H), 6.98 (d, J = 8.8 Hz, 2H), 4.01 (t, J = 6.5 Hz, 2H), 3.84 (t, J = 6.4 Hz, 2H), 1.96 (t, J = 7.3 Hz, 2H), 1.76–1.64 (m, 2H), 1.63–1.48 (m, 4H), 1.48–1.28 (m, 4H), 0.93 (t, J = 7.4 Hz, 3H) ppm. ^{13}C NMR (125.76 MHz, DMSO-d_6): δ = 168.92, 163.80, 161.13, 128.76, 124.22, 113.98, 74.97, 67.27, 32.10, 30.51, 27.37, 25.00, 24.83, 18.59, 13.58 ppm. IR (KBr): $\tilde{\nu}$ = 3220, 3120 (NH), 2935, 2871 (CH_2), 1619 (C=O) cm^{-1}. Anal. Calcd. for $C_{17}H_{26}N_2O_5$: C 60.34, H 7.74, N 8.28. Found: C 60.01, H 7.78, N 8.48.

4.3.5. N-((6-(Hydroxyamino)-6-oxohexyl)oxy)-4-propoxybenzamide (**1m**)

White solid; yield 32%; mp 112 °C. ^{1}H NMR (500.13 MHz, DMSO-d_6): δ = 11.48 (s, 1H), 10.37 (s, 1H), 8.68 (s, 1H), 7.71 (d, J = 8.7 Hz, 2H), 6.98 (d, J = 8.7 Hz, 2H), 3.97 (t, J = 6.5 Hz, 2H), 3.84 (t, J = 6.5 Hz, 2H), 1.96 (t, J = 7.4 Hz, 2H), 1.78–1.68 (m, 2H), 1.63–1.48 (m, 4H), 1.40–1.30 (m, 2H), 0.97 (t, J = 7.4 Hz, 3H) ppm. ^{13}C NMR (125.76 MHz, DMSO-d_6): δ = 168.89, 163.77, 161.09, 128.74, 124.19, 113.96, 74.95, 69.01, 32.09, 27.36, 24.99, 24.82, 21.82, 10.23 ppm. IR (KBr): $\tilde{\nu}$ = 3214 (NH), 2939, 2869 (CH_2), 1669 (C=O) cm^{-1}. Anal. Calcd. for $C_{16}H_{24}N_2O_5$: C 59.24, H 7.46, N 8.64. Found: C 59.45, H 7.56, N 8.42.

4.3.6. N-((6-(Hydroxyamino)-6-oxohexyl)oxy)-4-(pentyloxy) benzamide (**1n**)

White solid; yield 28%; mp 110 °C. ^{1}H NMR (500.13 MHz, DMSO-d_6): δ = 11.46 (s, 1H), 10.35 (s, 1H), 8.67 (s, 1H), 7.70 (d, J = 8.8 Hz, 2H), 6.98 (d, J = 8.8 Hz, 2H), 4.01 (t, J = 6.5 Hz, 2H), 3.84 (t, J = 6.5 Hz, 2H), 1.96 (t, J = 7.3 Hz, 2H), 1.77–1.67 (m, 2H), 1.63–1.48 (m, 4H), 1.46–1.27 (m, 6H), 0.89 (t, J = 7.1 Hz, 3H) ppm. ^{13}C NMR (125.76 MHz, DMSO-d_6): δ = 168.90, 163.76, 161.10, 128.74, 124.21, 113.97, 74.94, 67.54, 32.10, 28.15, 27.55, 27.37, 25.00, 24.82, 21.77, 13.81 ppm. IR (KBr): $\tilde{\nu}$ = 3211 (NH), 2940 (CH_2), 1672, 1616 (C=O) cm^{-1}. Anal. Calcd. for $C_{18}H_{28}N_2O_5$: C 61.34, H 8.01, N 7.95. Found: C 61.14, H 8.16, N 7.72.

4.3.7. 4-Ethoxy-N-((6-(hydroxyamino)-6-oxohexyl)oxy)benzamide (**1o**)

White solid; yield 25%; mp 125 °C. ^{1}H NMR (500.13 MHz, DMSO-d_6): δ = 11.46 (s, 1H), 10.35 (s, 1H), 8.67 (s, 1H), 7.71 (d, J = 8.8 Hz, 2H), 6.97 (d, J = 8.8 Hz, 2H), 4.07 (q, J = 7.0 Hz, 2H), 3.84 (t, J = 6.4 Hz, 2H), 1.96 (t, J = 7.3 Hz, 2H), 1.62–1.48 (m, 4H), 1.41–1.29 (m, 5H) ppm. ^{13}C NMR (125.76 MHz, DMSO-d_6): δ = 168.92, 163.79, 160.95, 128.76, 124.23, 113.94, 74.97, 63.20, 32.10, 27.36, 25.00, 24.82, 14.42 ppm. IR (KBr): $\tilde{\nu}$ = 3170 (NH), 2850 (CH_2), 1619 (C=O) cm^{-1}. Anal. Calcd. for $C_{15}H_{22}N_2O_5$: C 58.05, H 7.15, N 9.03. Found: C 57.81, H 7.25, N 8.97.

4.3.8. N-((6-(Hydroxyamino)-6-oxohexyl)oxy)-2-propoxybenzamide (**1p**)

White solid; yield 20%; mp 102 °C. ^{1}H NMR (500.13 MHz, DMSO-d_6): δ = 10.95 (s, 1H), 10.35 (s, 1H), 8.67 (s, 1H), 7.51–7.35 (m, 2H), 7.08 (d, J = 8.3 Hz, 1H), 6.99 (t, J = 7.4 Hz, 1H), 3.99 (t, J = 6.4 Hz, 2H), 3.85 (t, J = 6.5 Hz, 2H), 1.96 (t, J = 7.3 Hz, 2H), 1.80–1.68 (m, 2H), 1.66–1.47 (m, 4H), 1.42–1.27 (m, 2H), 0.98 (t, J = 7.4 Hz, 3H) ppm. ^{13}C NMR (125.76 MHz, DMSO-d_6): δ = 168.92, 163.20, 155.83, 131.65, 129.39, 122.91, 120.16, 112.59, 74.93, 69.54, 32.10, 27.24, 24.94, 24.84, 21.82, 10.32 ppm. IR (KBr): $\tilde{\nu}$ = 3349, 3230 (NH), 2936(CH_2), 1651 (C=O) cm^{-1}. HRMS (ESI) $[M + H]^+$: 325.17567, Calcd. for $C_{16}H_{25}N_2O_5$: 325.17580. HPLC analysis: retention time = 9.46 min; peak area: 97.52%. Eluent A: water; eluent B: methanol, gradient (50:50–>0:100) over 20 min at a flow rate of 1.0 mL min^{-1}.

4.3.9. N-((6-(Hydroxyamino)-6-oxohexyl)oxy)-3-propoxybenzamide (**1q**)

White solid; yield 14%; mp 101 °C. ^{1}H NMR (500.13 MHz, DMSO-d_6): δ = 11.61 (s, 1H), 10.36 (s, 1H), 8.68 (s, 1H), 7.44–7.22 (m, 3H), 7.09 (d, J = 6.9 Hz, 1H), 3.96 (t, J = 6.5 Hz, 2H), 3.86 (t, J = 6.2 Hz, 2H), 1.97 (t, J = 7.3 Hz, 2H), 1.79–1.68 (m, 2H), 1.64–1.49 (m, 4H), 1.42–1.30 (m, 2H), 0.99 (t, J = 7.4 Hz, 3H) ppm. ^{13}C NMR (125.76 MHz, DMSO-d_6): δ = 168.93, 163.74, 158.48, 133.63, 129.51, 119.06, 117.69, 112.60, 75.00, 69.00, 32.10, 27.35, 24.99, 24.82, 21.90, 10.29 ppm. IR (KBr): $\tilde{\nu}$ = 3210 (NH), 2938, 2874 (CH_2), 1670, 1624 (C=O) cm^{-1}. Anal. Calcd. for $C_{16}H_{24}N_2O_5$: C 59.24, H 7.46, N 8.64. Found: C 59.29, H 7.48, N 8.42.

4.3.10. 4-Butyl-N-((6-(hydroxyamino)-6-oxohexyl)oxy)benzamide (**1r**)

White solid; yield 20%; mp 119 °C. ^{1}H NMR (500.13 MHz, DMSO-d_6): δ = 11.54 (s, 1H), 10.36 (s, 1H), 8.68 (s, 1H), 7.66 (d, J = 8.1 Hz, 2H), 7.27 (d, J = 7.9 Hz, 2H), 3.85 (t, J = 6.5 Hz, 2H), 2.61 (t, J = 7.7 Hz, 2H), 1.96 (t, J = 7.4 Hz, 2H), 1.64–1.47 (m, 6H), 1.43–1.23 (m, 4H), 0.89 (t, J = 7.4 Hz, 3H) ppm. ^{13}C NMR (125.76 MHz, DMSO-d_6): δ = 168.90, 164.04, 146.11, 129.75, 128.19, 126.96, 74.97, 34.52, 32.75, 32.09, 27.35, 24.99, 24.82, 21.58, 13.64 ppm. IR (KBr): $\tilde{\nu}$ = 3205 (NH), 2943, 2865 (CH_2), 1650 (C=O) cm^{-1}. Anal. Calcd. for $C_{17}H_{26}N_2O_4$: C 63.33, H 8.13, N 8.69. Found: C 63.15, H 8.37, N 8.86.

4.3.11. 4-(Hexyloxy)-N-((6-(hydroxyamino)-6-oxohexyl)oxy) benzamide (**1s**)

White solid; yield 36%; mp 105 °C. ^{1}H NMR (500.13 MHz, DMSO-d_6): δ = 11.46 (s, 1H), 10.36 (s, 1H), 8.67 (s, 1H), 7.70 (d, J = 8.7 Hz, 2H), 6.98 (d, J = 8.8 Hz, 2H), 4.01 (t, J = 6.5 Hz, 2H), 3.84 (t, J = 6.4 Hz, 2H), 1.96 (t, J = 7.3 Hz, 2H), 1.76–1.65 (m, 2H), 1.63–1.47 (m, 4H), 1.46–1.23 (m, 8H), 0.88 (t, J = 6.9 Hz, 3H) ppm. ^{13}C NMR (125.76 MHz, DMSO-d_6): δ = 168.92, 163.80, 161.11, 128.75, 124.20, 113.98, 74.96, 67.56, 32.09, 30.86, 28.41, 27.54, 27.35, 25.02, 24.81, 21.95, 13.80 ppm. IR (KBr): $\tilde{\nu}$ = 3237 (NH), 2930 (CH_2), 1666, 1619 (C=O) cm^{-1}. Anal. Calcd. for $C_{19}H_{30}N_2O_5$: C 62.27, H 8.25, N 7.64. Found: C 62.38, H 8.40, N 7.35.

4.3.12. N-((6-(Hydroxyamino)-6-oxohexyl)oxy)furan-2-carboxamide (**1t**)

White solid; yield 32%; mp 113 °C. ^{1}H NMR (500.13 MHz, DMSO-d_6): δ = 11.61 (s, 1H), 10.35 (s, 1H), 8.67 (s, 1H), 7.85 (s, 1H), 7.09 (d, J = 3.1 Hz, 1H), 6.63 (dd, J = 3.1, 1.6 Hz, 1H), 3.83 (t, J = 6.4 Hz, 2H), 1.95 (t, J = 7.3 Hz, 2H), 1.65–1.45 (m, 4H), 1.39–1.27 (m, 2H) ppm. ^{13}C NMR (125.76 MHz, DMSO-d_6): δ = 168.95, 155.91, 145.60, 145.30, 113.89, 111.61, 75.36, 32.08, 27.29, 24.93, 24.80 ppm. IR (KBr): $\tilde{\nu}$ = 3250, 3137 (NH), 2936, 2867 (CH_2), 1666 (C=O) cm^{-1}. Anal. Calcd. for $C_{11}H_{16}N_2O_5$: C 51.56, H 6.29, N 10.93. Found: C 51.56, H 6.46, N 10.72.

4.3.13. 2-Fluoro-N-((6-(hydroxyamino)-6-oxohexyl)oxy)benzamide (**1u**)

Orange solid; yield 26%; mp 122 °C. ^{1}H NMR (500.13 MHz, DMSO-d_6): δ = 11.46 (s, 1H), 10.36 (s, 1H), 8.68 (s, 1H), 7.60–7.50 (m, 2H), 7.34–7.25 (m, 2H), 3.87 (t, J = 6.5 Hz, 2H), 1.96 (t, J = 7.4 Hz, 2H), 1.66–1.47 (m, 4H), 1.42–1.30 (m, 2H) ppm. ^{13}C NMR (125.76 MHz, DMSO-d_6): δ = 168.92, 160.99, 158.89 (d, $^1J_{C,F}$ = 249.2 Hz), 132.58 (d, $^3J_{C,F}$ = 8.4 Hz), 128.86 (d, $^4J_{C,F}$ = 3.1 Hz), 124.47 (d, $^3J_{C,F}$ = 3.6 Hz), 121.85 (d, $^2J_{C,F}$ = 15.6 Hz), 116.00 (d, $^2J_{C,F}$ = 21.9 Hz), 75.08, 32.09, 27.23, 24.91, 24.81 ppm. IR (KBr):

$\tilde{\nu}$ = 3297 (NH), 2949, 2878 (CH_2), 1673, 1635 (C=O) cm^{-1}. Anal. Calcd. for $C_{13}H_{17}FN_2O_4$: C 54.92, H 6.03, N 9.85. Found: C 55.05, H 6.31, N 9.65.

4.4. Asexual stage in vitro antimalarial assays

Activity against asexual stage *P. falciparum* line 3D7 was determined using [^{3}H]-hypoxanthine incorporation, essentially as previously described [29,38]. Serial dilutions of compounds were prepared in parasite culture media (RPMI 1640 supplemented with 10% heat inactivated human serum), followed by addition of synchronous ring-stage parasites 0.25% parasitaemia and 2.5% haematocrit. Following incubation for 48 h at 37 °C under standard parasite culture conditions, [^{3}H]-hypoxanthine (0.5 μCi/well) was added to each well, and the cultures incubated for a further 24 h. [^{3}H]-hypoxanthine incorporation was measured by harvesting onto 1450 MicroBeta filter mats (Wallac) and counting using a 1450 MicroBeta liquid scintillation counter. Percentage inhibition of growth compared to matched DMSO controls (0.5%) was determined. Three independent experiments were carried out, each in triplicate wells. Chloroquine was included in each assay as a positive control. IC_{50} values were determined using log-linear interpolation of inhibition curves [39] and are presented as mean (±SD) of the three independent assays.

4.5. Histone hyperacetylation assays

The effect of compounds on histone hyperacetylation was determined essentially as previously described [29]. Briefly, synchronous trophozoite-stage *P. falciparum* 3D7 parasites were incubated for 3 h under standard *in vitro* culture conditions with 500 nM of test compounds or vehicle control (0.05% DMSO). The antimalarial drug chloroquine (500 nM) was included as a negative control and TSA was included as a HDAC inhibitor positive control. Vehicle control samples were taken at the start (t = 0) and end (t = 3 h) of the treatment. Protein lysates were prepared by lysing cells with saponin (Sigma, USA) and extensive washing in phosphate buffered saline to remove haemoglobin. Parasite pellets were resuspended in SDS-PAGE loading dye, heat denatured at 96 °C then separated via 15% SDS-PAGE. Western blot was carried out using Odyssey reagents (LI-COR Biosciences) according to the manufacturers' instructions. The following primary antisera were used: anti-(tetra) acetyl H4 (Millipore) which recognizes lysines 5, 8, 12, and 16 of histone H4; anti-acetyl H3 which recognizes N-terminally acetylated histone H3; and anti-IC3/94 monoclonal antisera which was used as a loading control and recognizes *P. falciparum* rhoptry associated protein 2 (RAP2) [40]. IRDye® secondary antibodies (LI-COR Biosciences) were used and membranes imaged using an Odyssey infrared imaging system (LI-COR biosciences).

4.6. Deacetylase assays

Recombinant *Pf*HDAC1 (Sigma–Aldrich, USA) and *P. falciparum* nuclear protein lysates were tested for deacetylase activity using a fluorometric HDAC Assay Kit (Merck Millipore, USA), as per the manufacturers' instructions. Preparation of *P. falciparum* nuclear lysates from trophozoite stage parasites was carried out using a NucBuster protein extraction kit (Calbiochem, USA), according to the manufactures instructions. *Pf*HDAC1 activity was assessed using Fluorogenic HDAC substrate 3 (BPS Bioscience, USA). Assays were carried out in duplicate, on two separate occasions and data presented as mean (±SD) % inhibition compared to controls.

4.7. Late stage P. falciparum (IV–V) anti-gametocyte assay

Late stage gametocyte viability assays were carried out using highly synchronous stage IV gametocytes induced from transgenic NF54 *P. falciparum* parasites expressing the gametocyte specific protein, *Pfs*16, fused to green fluorescent protein (NF-54-pfs16-GFP), as described previously [41]. Gametocytes were harvested by magnetic isolation on day 8 post induction then added to 384 well imaging plates at 33,000 gametocytes per well. Following the addition of test or control compounds, cells were incubated for 72 h under reduced oxygen tension (5% CO_2, 5% O_2, 80% N_2). Mitotracker Red CM-H2XRos was then added to each well (0.07 ug/ml) and the cells were incubated overnight as described above. DMSO (0.4%) and puromycin (5 μM) were used as controls in each assay. Gametocyte viability was evaluated on an OPERA™ (PerkinElmer) High Content Screening System. Images acquired for GFP and Mitotracker Red CM-H2XRos were overlaid and the number of elongated viable gametocytes per image was determined using a script based on Acapella™ software, developed for use with the OPERA™ imaging system. Percent inhibition compared to DMSO vehicle controls was calculated and mean IC_{50} values (±SD) determined by non-linear regression analysis, sigmoidal dose response (variable slope) fit using Prizm 4.0 for two separate experiments in duplicate point.

4.7.1. Principle of script used for image analysis

Maximal fluorescent pixel intensities are identified for the MTR acquired image and the average intensity for designated objects calculated. Objects with an average fluorescent MTR intensity, above an assay specified classification of minimal MTR signal, are identified as viable objects. GFP positive objects are identified and overlaid with the MTR positive objects. The GFP objects with a MTR positive signal are then evaluated for the characteristic of being at least four times longer than they are wide. Objects that are both MTR positive and GFP object elongated are identified as viable late stage gametocytes.

4.8. Pb liver stage assay

4.8.1. Parasites

P. berghei Luciferase sporozoites from MR4 (MRA-868) [42] were obtained by dissection of infected *Anopheles stephensi* mosquito salivary glands. Dissected salivary glands were homogenized in a glass tissue grinder and filtered twice through nylon cell strainers (40 μm pore size, BD Falcon 087711) and counted using a haemocytometer. The sporozoites were kept on ice until needed.

4.8.2. Cell lines

HepG2-A16-CD81EGFP cells stably transformed to express a GFP-CD81 fusion protein [43] were cultured at 37 °C in 5% CO_2 in DMEM (Invitrogen, Carlsbad, USA) supplemented with 10% FCS, and 1× Penicillin-Streptomycin-Glutamine (Gibco, Life Technologies, USA).

4.8.3. Sporozoite infection

We used *P. berghei* for this screen since its higher infection rates of immortal human liver cell lines are more conducive to high throughput screening than the infection rates of human malaria parasites. *P. berghei* is able to infect human hepatocarcinoma HepG2 cells expressing the tetraspanin CD81 receptor [43,44]. 3 × 10^3 HepG2-A16-CD81EGFP cells in 5 μl of medium (2 × 10^5 cells/ml, 5% FBS, 5× Penicillin-Streptomycin-Glutamine (Gibco, Life Technologies, USA)) were seeded in 1536-well plates (Greiner BioOne white solid bottom, custom GNF mold) 20–26 h prior to the actual infection. 18 h prior to infection, 50 nl of

compound in DMSO (0.5% final DMSO concentration per well) were transferred with a PinTool (GNF Systems) or Echo liquid handler (LabCyte) into the assay plates. Atovaquone (12-point serial dilution starting at 10 μM) and 0.5% DMSO were used as positive and negative controls, respectively. *P. berghei* Luciferase sporozoites were freshly dissected as described above and their concentration adjusted to 200 sporozoites per μl (final concentration: 1000 sporozoites per well) with 5× Penicillin-Streptomycin-Glutamine (Gibco, Life Technologies, USA) in DMEM (Invitrogen). The increased antibiotic concentration did not interfere with the parasite or HepG2-A16-CD81EGFP growth. The HepG2-A16-CD81EGFP cells were then infected with 1×10^3 sporozoites per well (5 μl) with a single tip Bottle Valve liquid handler (GNF Systems), and the plates spun down at 37 °C for 3 min in an Eppendorf 5810 R centrifuge with a centrifugal force of 330× g on lowest acceleration and brake setting. The plates were then incubated at 37 °C for 48 h in 5% CO_2 with high humidity to minimize media evaporation and edge effect. After incubation, media was removed by spinning the inverted plates at 150× g for 30 s 2 μl BrightGlo luciferase (Promega) were dispensed with the MicroFlo (BioTek) liquid handler. Immediately after addition of the luminescence reagent, the plates were vortexed at median intensity setting for 10 s and read by an EnVision Multilabel Reader (PerkinElmer). IC_{50} values were determined using a non-linear variable slope four parameter regression curve fitting model in Prism 6 (GraphPad Software Inc).

4.8.4. HepG2 toxicity assay

HepG2 viability after 56 h was used to assess compound toxicity. Specifically we assayed ATP levels of live HepG2 host cells and compared them to ATP levels of DMSO-treated control cells. Hepatocytes were cultured as described above, but on the day of infection, instead of sporozoites, 5 μl media was added with a MicroFlo (BioTek) liquid handler. After the 48 h incubation period, media was removed by spinning the inverted plates at 150× g for 30 s 2 μl of CellTiterGlo (Promega) diluted 1:1 with ddH_2O were dispensed with the MicroFlo (BioTek) liquid handler and read by an EnVision Multilabel Reader (PerkinElmer). IC_{50} values were determined as described above (Section 4.8.3).

Funding sources

This work was supported by the Australian Research Council (FT0991213 to KTA; LP120200557 to VMA), Medicines for Malaria Ventures (MMV) (to SM and VMA) as well as the Bill and Melinda Gates Foundation, MMV, and NIH (R01AI090141) (to EAW).

Acknowledgements

We thank the Australian Red Cross Blood Service for the provision of human blood and sera. The Deutsche Forschungsgemeinschaft (DFG) is acknowledged for funds used to purchase the UHR-TOF maXis 4G, Bruker Daltonics, Bremen HRMS instrument used in this research.

Appendix A. Supplementary data

Supplementary data related to this article can be found at http://dx.doi.org/10.1016/j.ejmech.2014.05.050.

References

[1] World Health Organization, World Malaria Report 2011, WHO Press, Geneva, 2012.
[2] C.J. Murray, L.C. Rosenfeld, S.S. Lim, K.G. Andrews, K.J. Foreman, D. Haring, N. Fullman, M. Naghavi, R. Lozano, A.D. Lopez, Global malaria mortality between 1980 and 2010: a systematic analysis, Lancet 379 (2012) 413–431.
[3] S. Abdulla, N. Salim, F. Machera, R. Kamata, O. Juma, M. Shomari, S. Kubhoja, A. Mohammed, G. Mwangoka, T. Aebi, H. Mshinda, D. Schellenberg, T. Carter, T. Villafana, M.-C. Dubois, A. Leach, M. Lievens, J. Vekemans, J. Cohen, W.R. Ballou, M. Tanner, Randomized, controlled trial of the long term safety, immunogenicity and efficacy of RTS,S/AS02(D) malaria vaccine in infants living in a malaria-endemic region, Malar. J. 12 (2013) 11.
[4] S.T. Agnandji, B. Lell, S.S. Soulanoudjingar, J.F. Fernandes, B.P. Abossolo, C. Conzelmann, B.G. Methogo, Y. Doucka, A. Flamen, B. Mordmüller, S. Issifou, P.G. Kremsner, J. Sacarlal, P. Aide, M. Lanaspa, J.J. Aponte, A. Nhamuave, D. Quelhas, Q. Bassat, S. Mandjate, E. Macete, P. Alonso, S. Abdulla, N. Salim, O. Juma, M. Shomari, K. Shubis, F. Machera, A.S. Hamad, R. Minja, A. Mtoro, A. Sykes, S. Ahmed, A.M. Urassa, A.M. Ali, G. Mwangoka, M. Tanner, H. Tinto, U. D'Alessandro, H. Sorgho, I. Valea, M.C. Tahita, W. Kabore, S. Ouedraogo, Y. Sandrine, R.T. Guiguemde, J.B. Ouedraogo, M.J. Hamel, S. Kariuki, C. Odero, M. Oneko, K. Otieno, N. Awino, J. Omoto, J. Williamson, V. Muturi-Kioi, K.F. Laserson, L. Slutsker, W. Otieno, L. Otieno, O. Nekoye, S. Gondi, A. Otieno, B. Ogutu, R. Wasuna, V. Owira, D. Jones, A.A. Onyango, P. Njuguna, R. Chilengi, P. Akoo, C. Kerubo, J. Gitaka, C. Maingi, T. Lang, A. Olotu, B. Tsofa, P. Bejon, N. Peshu, K. Marsh, S. Owusu-Agyei, K.P. Asante, K. Osei-Kwakye, O. Boahen, S. Ayamba, K. Kayan, R. Owusu-Ofori, D. Dosoo, I. Asante, G. Adjei, D. Chandramohan, B. Greenwood, J. Lusingu, S. Gesase, A. Malabeja, O. Abdul, H. Kilavo, C. Mahende, E. Liheluka, M. Lemnge, T. Theander, C. Drakeley, D. Ansong, T. Agbenyega, S. Adjei, H.O. Boateng, T. Rettig, J. Bawa, J. Sylverken, D. Sambian, A. Agyekum, L. Owusu, F. Martinson, I. Hoffman, T. Mvalo, P. Kamthunzi, R. Nkomo, A. Msika, A. Jumbe, N. Chome, D. Nyakuipa, J. Chintedza, W.R. Ballou, M. Bruls, J. Cohen, Y. Guerra, E. Jongert, D. Lapierre, A. Leach, M. Lievens, O. Ofori-Anyinam, J. Vekemans, T. Carter, D. Lebouleux, C. Loucq, A. Radford, B. Savarese, D. Schellenberg, M. Sillman, P. Vansadia, First results of phase 3 trial of RTS,S/AS01 malaria vaccine in African children, N. Engl. J. Med. 365 (2011) 1863–1875.
[5] S. Turschner, T. Efferth, Drug resistance in Plasmodium: natural products in the fight against malaria, Mini Rev. Med. Chem. 9 (2009) 206–214.
[6] A.M. Dondorp, F. Nosten, P. Yi, D. Das, A.P. Phyo, J. Tarning, K.M. Lwin, F. Ariey, W. Hanpithakpong, S.J. Lee, P. Ringwald, K. Silamut, M. Imwong, K. Chotivanich, P. Lim, T. Herdman, S.S. An, S. Yeung, P. Singhasivanon, N.P. Day, N. Lindegardh, D. Socheat, N.J. White, Artemisinin resistance in *Plasmodium falciparum* malaria, N. Engl. J. Med. 361 (2009) 455–467.
[7] A.M. Dondorp, S. Yeung, L. White, C. Nguon, N.P. Day, D. Socheat, L. von Seidlein, Artemisinin resistance: current status and scenarios for containment, Nat. Rev. Microbiol. 8 (2010) 272–280.
[8] The malERA Consultative Group on Drugs, A research agenda for malaria eradication: drugs, PLoS Med. 8 (2011) e1000402.
[9] J.N. Burrows, Antimalarial drug discovery: where next? Future Med. Chem. 4 (2012) 2233–2235.
[10] T. Rodrigues, M. Prudêncio, R. Moreira, M.M. Mota, F. Lopes, Targeting the liver stage of malaria parasites: a yet unmet goal, J. Med. Chem. 55 (2012) 995–1012.
[11] O. Dechy-Cabaret, F. Benoit-Vical, Effects of antimalarial molecules on the gametocyte stage of *Plasmodium falciparum*: the debate, J. Med. Chem. 55 (2012) 10328–10344.
[12] L. Lucantoni, V. Avery, Whole-cell in vitro screening for gametocytocidal compounds, Future Med. Chem. 4 (2012) 2337–2360.
[13] K.T. Andrews, T.N. Tran, D.P. Fairlie, Towards histone deacetylase inhibitors as new antimalarial drugs, Curr. Pharm. Des. 18 (2012) 3467–3479.
[14] K.T. Andrews, T.N. Tran, N.C. Wheatley, D.P. Fairlie, Targeting histone deacetylase inhibitors for anti-malarial therapy, Curr. Top. Med. Chem. 9 (2009) 292–308.
[15] M. Biel, V. Wascholowski, A. Giannis, Epigenetics – an epicenter of gene regulation: histones and histone-modifying enzymes, Angew. Chem. Int. Ed. 44 (2005) 3186–3216.
[16] P. Bertrand, Inside HDAC with HDAC inhibitors, Eur. J. Med. Chem. 45 (2010) 2095–2116.
[17] O. Witt, H.E. Deubzer, T. Milde, I. Oehme, HDAC family: what are the cancer relevant targets? Cancer Lett. 277 (2009) 8–21.
[18] W.S. Xu, R.B. Parmigiani, P.A. Marks, Histone deacetylase inhibitors: molecular mechanisms of action, Oncogene 26 (2007) 5541–5552.
[19] X.-J. Yang, E. Seto, HATs and HDACs: from structure, function and regulation to novel strategies for therapy and prevention, Oncogene 26 (2007) 5310–5318.
[20] S. Balasubramanian, E. Verner, J.J. Buggy, Isoform-specific histone deacetylase inhibitors: the next step? Cancer Lett. 280 (2009) 211–221.
[21] O. Khan, N.B. La Thangue, HDAC inhibitors in cancer biology: emerging mechanisms and clinical applications, Immunol. Cell. Biol. 90 (2012) 85–94.
[22] P. Horrocks, E. Wong, K. Russell, R.D. Emes, Control of gene expression in *Plasmodium falciparum* – ten years on, Mol. Biochem. Parasitol. 164 (2009) 9–25.
[23] V. Patel, R. Mazitschek, B. Coleman, C. Nguyen, S. Urgaonkar, J. Cortese, R.H. Barker, E. Greenberg, W. Tang, J.E. Bradner, S.L. Schreiber, M.T. Duraisingh, D.F. Wirth, J. Clardy, Identification and characterization of small molecule inhibitors of a class I histone deacetylase from *Plasmodium falciparum*, J. Med. Chem. 52 (2009) 2185–2187.
[24] G. Hu, A. Cabrera, M. Kono, S. Mok, B.K. Chaal, S. Haase, K. Engelberg, S. Cheemadan, T. Spielmann, P.R. Preiser, T.-W. Gilberger, Z. Bozdech, Transcriptional profiling of growth perturbations of the human malaria parasite *Plasmodium falciparum*, Nat. Biotechnol. 28 (2010) 91–98.
[25] K.T. Andrews, A.P. Gupta, T.N. Tran, D.P. Fairlie, G.N. Gobert, Comparative gene expression profiling of *P. falciparum* malaria parasites exposed to three different histone deacetylase inhibitors, PLoS ONE 7 (2012) e31847.

[26] B.K. Chaal, A.P. Gupta, B.D. Wastuwidyaningtyas, Y.-H. Luah, Z. Bozdech, Histone deacetylases play a major role in the transcriptional regulation of the *Plasmodium falciparum* life cycle, PLoS Pathog. 6 (2010) e1000737.
[27] S. Mok, M. Imwong, M.J. Mackinnon, J. Sim, R. Ramadoss, P. Yi, M. Mayxay, K. Chotivanich, K.-Y. Liong, B. Russell, D. Socheat, P.N. Newton, N.P.J. Day, N.J. White, P.R. Preiser, F. Nosten, A.M. Dondorp, Z. Bozdech, Artemisinin resistance in *Plasmodium falciparum* is associated with an altered temporal pattern of transcription, BMC Gen. 12 (2011) 391.
[28] G.S. Dow, Y. Chen, K.T. Andrews, D. Caridha, L. Gerena, M. Gettayacamin, J. Johnson, Q. Li, V. Melendez, N. Obaldia, T.N. Tran, A.P. Kozikowski, Antimalarial activity of phenylthiazolyl-bearing hydroxamate-based histone deacetylase inhibitors, Antimicrob. Ag. Chemother. 52 (2008) 3467–3477.
[29] S.D.M. Sumanadasa, C.D. Goodman, A.J. Lucke, T. Skinner-Adams, I. Sahama, A. Haque, T.A. Do, G.I. McFadden, D.P. Fairlie, K.T. Andrews, Antimalarial activity of the anticancer histone deacetylase inhibitor SB939, Antimicrob. Ag. Chemother. 56 (2012) 3849–3856.
[30] L. Marek, A. Hamacher, F.K. Hansen, K. Kuna, H. Gohlke, M.U. Kassack, T. Kurz, Histone deacetylase (HDAC) inhibitors with a novel connecting unit linker region reveal a selectivity profile for HDAC4 and HDAC5 with improved activity against chemoresistant cancer cells, J. Med. Chem. 56 (2013) 427–436.
[31] V. Duléry, O. Renaudet, P. Dumy, Ethoxyethylidene protecting group prevents *N*-overacylation in aminooxy peptide synthesis, Tetrahedron 63 (2007) 11952–11958.
[32] S. Foillard, M.O. Rasmussen, J. Razkin, D. Boturyn, P. Dumy, 1-Ethoxyethylidene, a new group for the stepwise SPPS of aminooxyacetic acid containing peptides, J. Org. Chem. 73 (2008) 983–991.
[33] B. Draghici, F.K. Hansen, A.-M. Buciumas, B.E.-D.M. El-Gendy, E. Todadze, A.R. Katritzky, Efficient microwave-assisted synthesis of aminoxy acid conjugates, RSC Adv. 1 (2011) 602–606.
[34] C. Jiménez-Castells, B.G. de la Torre, R. Gutiérrez Gallego, D. Andreu, Optimized synthesis of aminooxy-peptides as glycoprobe precursors for surface-based sugar-protein interaction studies, Bioorg. Med. Chem. Lett. 17 (2007) 5155–5158.
[35] C.A. Lipinski, F. Lombardo, B.W. Dominy, P.J. Feeney, Experimental and computational approaches to estimate solubility and permeability in drug discovery and development settings, Adv. Drug. Deliv. Rev. 46 (2001) 3–26.
[36] F.K. Hansen, T.S. Skinner-Adams, S. Duffy, L. Marek, S.D.M. Sumanadasa, K. Kuna, J. Held, V.M. Avery, K.T. Andrews, T. Kurz, Synthesis, antimalarial properties and SAR studies of alkoxyurea-based HDAC inhibitors, ChemMedChem 9 (2014) 665–670.
[37] B. Jones, The halogenation of phenolic ethers and anilides. Part XIV. *m*-substituted phenyl ethers, J. Chem. Soc. (1943) 430–432.
[38] R.E. Desjardins, C.J. Canfield, J.D. Haynes, J.D. Chulay, Quantitative assessment of antimalarial activity in vitro by a semiautomated microdilution technique, Antimicrob. Ag. Chemother. 16 (1979) 710–718.
[39] W. Huber, J.C. Koella, A comparison of three methods of estimating EC50 in studies of drug resistance of malaria parasites, Acta Trop. 55 (1993) 257–261.
[40] D.L. Baldi, K.T. Andrews, R.F. Waller, D.S. Roos, R.F. Howard, B.S. Crabb, A.F. Cowman, RAP1 controls rhoptry targeting of RAP2 in the malaria parasite *Plasmodium falciparum*, EMBO J. 19 (2000) 2435–2443.
[41] S. Duffy, V.M. Avery, Identification of inhibitors of *Plasmodium falciparum* gametocyte development, Malar. J. 12 (2013) 408.
[42] C.J. Janse, B. Franke-Fayard, G.R. Mair, J. Ramesar, C. Thiel, S. Engelmann, K. Matuschewski, G.J. van Gemert, R.W. Sauerwein, A.P. Waters, High efficiency transfection of *Plasmodium berghei* facilitates novel selection procedures, Mol. Biochem. Parasitol. 145 (2006) 60–70.
[43] S. Yalaoui, S. Zougbédé, S. Charrin, O. Silvie, C. Arduise, K. Farhati, C. Boucheix, D. Mazier, E. Rubinstein, P. Froissard, Hepatocyte permissiveness to *Plasmodium* infection is conveyed by a short and structurally conserved region of the CD81 large extracellular domain, PLoS Pathog. 4 (2008) e1000010.
[44] O. Silvie, E. Rubinstein, J.-F. Franetich, M. Prenant, E. Belnoue, L. Rénia, L. Hannoun, W. Eling, S. Levy, C. Boucheix, D. Mazier, Hepatocyte CD81 is required for *Plasmodium falciparum* and *Plasmodium yoelii* sporozoite infectivity, Nat. Med. 9 (2003) 93–96.